COMPUTATIONAL MECHANICS 2021
36th conference with international participation
Srní
November 8 - 10, 2021

Macroscopic constitutive model for NiTi shape memory alloys: Formulation, numerical implementation, and application in materials research

M. Frost, P. Sedlák

Institute of Thermomechanics, Czech Academy of Sciences, Dolejškova 5,182 00 Praha, Czech Republic

1. Introduction

Shape memory alloys (SMA) are metallic materials with the ability to undergo reversible phase solid-to-solid phase transformation between a high-symmetry and a low-symmetry phase. In addition to temperature variation, the phase transition may be induced by applying stress on the high-symmetry phase. The most common and practically utilized example are the alloys with nickel and titanium as the dominant constituents, known as NiTi-based SMA.

From the viewpoint of mechanics, an exciting feature of NiTi SMA polycrystals is the ability to be strained up to 10% deformation and, after unloading, to fully recover the original shape; this is called *superelasticity*, and it manifests itself at higher temperatures. If the material is deformed at low temperatures and then its shape-change is constrained, it generates relatively high force (called recovery force) against the constraint. Finally, loaded SMA structure can perform work when cycled between high and low temperatures.

All these features gave rise to many smart and useful applications of NiTi SMA [5]. It is not surprising that soon after their discovery, SMA attracted the attention of a wide engineering community. Since 1980s, there has been a continuous effort to develop a complex constitutive model capable of reproducing the specific mechanical response. Because of many additional peculiarities, e.g., the pronounced asymmetry of the response in tension and compression, anisotropy of some physical properties, or the inclination towards strain localization, a robust and comprehensive constitutive model tailored even for the commercially most successful NiTi alloy is still sought.

2. Constitutive model and its numerical implementation into finite element software

The inherent challenge for constitutive modeling is that multiple microstructural processes can be simultaneously activated in the material, and these processes are mutually interdependent, i.e., activation of one process can influence the progress of another one and *vice versa*. Most of them are *dissipative*, which indicates thermodynamic irreversibility. For such situations, continuum thermodynamics offers some powerful modeling tools. The model presented in this contribution is developed within the so-called *generalized standard materials* framework [4], which employs only two potential functions – energy function and dissipation function – as determinants for the complete evolution of the system. So-called internal (state) variables serving as the descriptors of the present material state complement the conventional state variables (e.g. strain and temperature) in the functions' definitions. Let us note that the particular choice

of internal variables and the form of the two functions are tightly linked to the knowledge and understanding of the material system by the authors of the model.

The constitutive (evolutionary) equations are determined via a mathematical relation between generalized forces obtained from the energy function and (generalized) gradients of the dissipation function. Under some (relatively weak) conditions, this relation may be derived from a suitable thermodynamic extremum principle [3]. The variational character of the framework then allows for the exploitation of incremental energy minimization approaches in the numerical implementation of the model.

The numerical implementation of the boundary value problems typical for computational mechanics involves a spatial discretization (the finite element method is usually the first-choice tool) and a temporal discretization. For the common backward Euler implicit scheme, the latter corresponds to a time-incremental problem of determining the state-update of the material at a time instant t_{n+1} based on the known state at the time instant t_n and some prescribed disturbance of that state. The microstructural processes behind the characteristic effects of SMA (athermal phase transformation, crystal twinning) are, similarly to the conventional flow plasticity, in a good approximation *rate-independent* (i.e., the dissipation function is homogenous first order in rates of internal variables). Most of the common methods for the solution of the resulting time-incremental problem can be classified as "check and treat" strategy: first, the possibility that the inelastic process is not active is checked and, if it is not the case, the process is considered as active, and the evolution is resolved. These methods are usually quite flexible and easy to implement; however, with an increasing number of involved inelastic processes and their mutual coupling, searching for the set of active processes turns into a complex and elaborate task.

The minimization problems stemming from the variational formulation can also be dealt with "check and treat" strategies; however, they also allow for employing direct minimization procedures or algorithms of mathematical programming. The former option was used for resolving the constitutive equations of the model introduced in [6], implemented within the user material (UMAT) subroutine of the commercial finite element solver Abaqus, and it has been successfully employed in three-dimensional computational simulations as demonstrated on the example in the following section.

3. Computational simulation of experiments on NiTi helical spring

A computational simulation employing the constitutive model [6] was used as a tool for analysis and interpretation of experimental data obtained on a NiTi helical spring by diffraction/scanning computational tomography. Let us note that this experimental method allows for in situ reconstruction of the spatial distribution of microstructural heterogeneities within probed samples, see details in [1]. A helical spring was chosen as the object of this study since it allows for simple manufacturing and direct utilization in actuating devices and, at the same time, when stretched to higher strokes, two deformation modes – twisting and bending – are simultaneously active and naturally result in a heterogeneous, non-proportional deformation within any cross-section.

In the experimental part, a helical spring was manufactured from a NiTi wire, its superelastic response (at room temperature) was measured (see the upper inset in Fig. 1), and a series of X-ray diffraction scanning runs was performed at two distinct deformation states, denoted S1 and S2 hereinafter. The computational tomography algorithms were then employed to resolve the spatial distribution of volume fractions of phases in the cross-section of the spring at the two states (see Fig. 2). More details can be found in [2].

In the computational simulation, a structural model of a one-coil spring (dimensions corre-

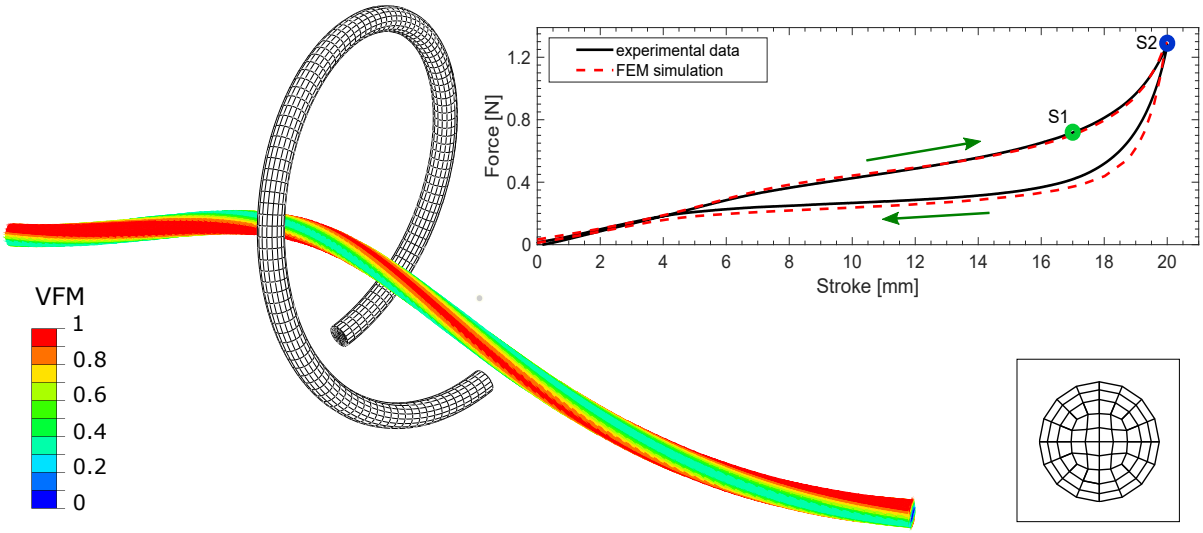

Fig. 1. Finite element model of the helical spring. The free-standing mesh is in grey; the mesh layout in an arbitrary cross-section is shown in the lower inset. The deformed configuration corresponding to the maximum stroke (S2) is in colors displaying the computed volume fraction of the low-symmetry phase (see the colorbar). The upper inset (graph) compares measured (black line) and simulated (red dashed line) dependence of total force on stroke obtained from the FE simulation. Marked points S1 and S2 correspond to strokes at which the diffraction scanning was performed

spond to the spring used in experiments) was constructed and meshed into 120 equivalent cross-sectional element layers with 64 elements per layer. In Fig. 1, the complete mesh is depicted on the undeformed configuration; the arrangement of 64 elements within an arbitrary layer is shown in the lower square inset. The computation was performed with eight-node linear hexaedral elements with centroid integration (C3D8R). Geometric nonlinearities were accounted for via *NLGEOM settings. Stretching of the spring was simulated by a gradual, symmetrical change of prescribed x-displacement (parallel with the coil axis) of the central nodes at both ends of the coil, displacement in other directions of these nodes were fixed, and the rigid body motion of the whole coil was prevented. The periodic boundary conditions with shifted x-displacement are imposed via *EQUATION functionality of Abaqus FEA at the remaining nodes of both ends of the segment (infinite spring approximation). Material parameters serving as the model's input were determined from a standardized experimental dataset measured on the constituent wire.

Fig. 1 also shows the deformed configuration of the coil corresponding to the maximum stretch of the real spring (S2). The distribution of computed volume fraction of martensite on the wire surface (see the colorbar) complies with the symmetry of the model. The upper inset compares the force-stroke response obtained in the experiment (black line) with the simulation (red dashed line). The overall excellent match is observed (with respect to experimental errors).

The main aim of the computational part was to reveal the spatial distribution of the quantities representing volume fractions of phases within the cross-section of the spring so that it can be directly compared with the results of the computational tomography employing the diffraction experiment. This comparison is presented in Fig. 2 for the volume fraction of the high-symmetry phase (austenite) denoted as VFA there. Distributions are shown for both deformation stages S1 and S2. Let us note that the inclination of the spring wire to the probing plane results in the ellipticity of the cross-sections.

The comparison of results provides valuable information from the computational modeling point of view. First, it confirms plausible parametrization of the model via the internal variables:

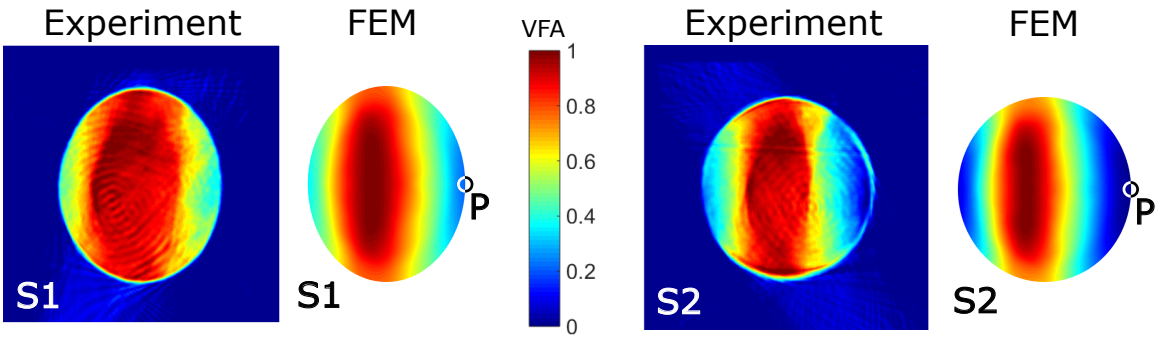

Fig. 2. Spatial distribution of the volume fraction of austenite (VFA) within the spring cross-section determined from scanning experiments compared with its equivalent computed in the finite element simulation (an arbitrary cross-section of the structural model) at two deformation states S1 and S2 (cf. Fig. 1). The same colorbar applies to all phase distributions. The coil axis is directly to the right from the center of the cross-sections; hence, point P lies on the most inner material fiber of the coil

phase gradients existing in the material are very well (considering also experimental errors) detected and even quantified by the model. Second, the main features of the phase pattern can be interpreted in the terms of advanced features of the model; e.g. the obvious asymmetry of the pattern with respect to the "neutral axis" of bending is due to the so-called tension-compression asymmetry of the material response implemented in the model. Third, the variation of the model parameters can help determine the physical characteristics (parameters) of the material which can be difficult to obtain directly through experiments. For instance, the tension-compression asymmetry parameter can be obtained via its variation in the model so that the best correspondence between the simulation and experimental patterns is reached. Finally, the model provides distributions of state variables, e.g., components of the stress tensor, which are difficult or even impossible to gain through conventional experimental techniques.

Acknowledgements

The financial support via project No. GA18-03834S provided by the Czech Science Foundation is acknowledged as well as the provision of experimental beamtime at the beamline ID 15A within experiment No. MA2114 by European Synchrotron Radiation Facility in France.

References

[1] Àlvarez-Murga, M., Bleuet, P., Hodeau, J., Diffraction/scattering computed tomography for three-dimensional characterization of multi-phase crystalline and amorphous materials, Journal of Applied Crystallography 45 (6) (2012) 1109-1124.

[2] Frost, M., Ševčík, M., Kadeřávek, L., Šittner, P., Sedlák, P., Reconstruction of phase distributions in NiTi helical spring: comparison of diffraction/scattering computed tomography and computational modeling, Smart Materials and Structures 29 (2020) No. 075036.

[3] Hackl, K., Fischer, F. D., On the relation between the principle of maximum dissipation and inelastic evolution given by dissipation potentials, Proceedings of The Royal Society A – Mathematical Physical and Engineering Sciences 464 (2008) 117-132.

[4] Halphen, B., Nguyen, Q. S., On generalized standard materials, Journal de Mécanique 14 (1975) 39-63. (in French)

[5] Mohd Jani, J., Leary, M., Subic, A., Gibson, M. A., A review of shape memory alloy research, applications and opportunities, Materials & Design 56 (2014) 1078-1113.

[6] Sedlák, P., Frost, M., Benešová, B., Šittner, P., Ben Zineb, T., Thermomechanical model for NiTi-based shape memory alloys including R-phase and material anisotropy under multi-axial loadings, International Journal of Plasticity 39 (2012) 132-151.